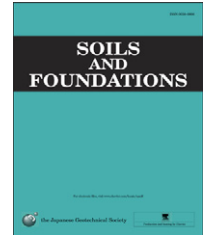




The Japanese Geotechnical Society

Soils and Foundations

www.sciencedirect.com
journal homepage: www.elsevier.com/locate/sandf



Stiffness and strength parameters for hardening soil model of soft and stiff Bangkok clays

Chanaton Surarak^a, Suched Likitlersuang^{b,*}, Dariusz Wanatowski^c,
Arumugam Balasubramaniam^a, Erwin Oh^a, Hong Guan^a

^aGriffith School of Engineering, Griffith University Gold Coast Campus, Queensland 4222, Australia

^bDepartment of Civil Engineering, Faculty of Engineering, Chulalongkorn University, Phayathai Road, Pathumwan Bangkok, 10330 Thailand

^cNottingham Centre for Geomechanics, Faculty of Engineering, University of Nottingham, United Kingdom

Received 20 June 2011; received in revised form 30 April 2012; accepted 19 June 2012

Available online 7 September 2012

Abstract

A comprehensive set of experimental data on Bangkok subsoils from oedometer and triaxial tests are analysed in this paper in order to determine the stiffness and strength parameters for Hardening Soil Model. The parameters determined are the Mohr–Coulomb effective stress strength parameters together with the stiffness parameters; tangent stiffness for primary oedometer loading, secant stiffness in undrained and drained triaxial tests, unloading/reloading stiffness and the power for stress level dependency of stiffness. The oedometer data are obtained from three different Bangkok soil layers: soft clay at 6–8 m depths; medium clay at 12–14 m depths; and stiff clay at 15.5–18 m depths. The triaxial tests data are carried out for soft and stiff clays at depths of 5.5–6 m and of 16–18 m under both undrained and drained conditions, respectively. Finally, two sets of parameters for soft and stiff Bangkok clays are numerically calibrated against undrained and drained triaxial results using PLAXIS finite element software.

© 2012 The Japanese Geotechnical Society. Production and hosting by Elsevier B.V. All rights reserved.

Keywords: Stiffness parameters; Hardening soil model; Bangkok clay; Oedometer test; Triaxial test; Finite element method

1. Introduction

Bangkok subsoils are one of the most well-known sedimentary soils and have been studied extensively in the past by many research students at the Asian Institute of

Technology under the supervision of the fourth author (see Chaudhry, 1975; Li, 1975; Hwang, 1975; Ahmed, 1976; Hassan, 1976; Kim, 1990; Gurung, 1992). The experimental work was on isotropically and anisotropically consolidated triaxial tests both in compression and in extension. The results were primarily used to verify the critical state theories as developed for normally and overconsolidated clays (Balasubramaniam and Chaudhry, 1978; Balasubramaniam et al., 1978, 1992; Balasubramaniam and Hwang, 1980). Additionally, full scale field tests on embankments and excavations were modelled using CRISP finite element programme. Subsequently user friendly computer software such as PLAXIS was found to be more versatile for using in practice than the CRISP. In a doctoral thesis by Surarak (2010), soil models used in PLAXIS such as the Mohr–Coulomb Model, the Hardening Soil Model, and the

*Corresponding author.

E-mail addresses: chanatons@gmail.com (C. Surarak),
suched.l@eng.chula.ac.th (S. Likitlersuang),
dariusz.wanatowski@nottingham.ac.uk (D. Wanatowski),
a.bala@griffith.edu.au (A. Balasubramaniam),
E.Oh@griffith.edu.au (E. Oh), h.guan@griffith.edu.au (H. Guan).

Peer review under responsibility of The Japanese Geotechnical Society.



Hardening Soil Model with Small Strain Behaviour were studied in great detail to have better knowledge on their practical applications such as in the design and performance of deep excavations and tunnelling works in Bangkok MRT project. This paper presents only the work on stiffness and strength parameters for the Hardening Soil Model.

In the Hardening Soil Model, oedometer tests and triaxial tests data are used. The oedometer test data are studied for soft Bangkok clay at 6–8 m depths; medium clay at 12–14 m depths; and stiff clay at 15.5–18 m depths. The triaxial test data are on soft and stiff clays at depths of 3–4 m and of 16–18 m, respectively. The Mohr–Coulomb strength parameters c' and ϕ' are obtained from triaxial tests conducted both under undrained and drained conditions. The stiffness parameter E_{oed}^{ref} is determined from oedometer tests on both soft and stiff Bangkok clays. The secant stiffness E_{50}^{ref} is obtained from both undrained and drained triaxial tests on soft and stiff Bangkok clays. The unloading/reloading stiffness parameter $E_{ur, oed}^{ref}$ is also determined from oedometer tests. The power (m) for stress level dependency of stiffness is determined from both oedometer and triaxial tests. Finally, finite element modelling of triaxial and oedometer tests is carried out to calibrate and verify the stiffness parameters determined from the laboratory tests.

2. Bangkok sub-soil conditions

Bangkok is situated on the flood plain and delta of the Chao Phraya River, which traverses the Lower Central Plain of Thailand (Fig. 1). The Quaternary deposits of the Lower Central Plain represent a complex sequence of alluvial, fluvial and deltaic sediments. The Quaternary stratigraphy consists of eight aquifers: Bangkok (BK), Phrapadang (PD), Nakornluang (NL), Nonthaburi (NB), Sam Khok (SK), Phaya Thai (PT), Thonburi (TB) and Pak Nam (PN) aquifers. They are separated from each other by thick layers of clay or sandy clay. The depth of the bedrock is still undetermined, but its level in the Bangkok area is known to vary between 400 m to 1,800 m depth. Deep well pumping from the aquifers over the last fifty years or so has caused substantial piezometric draw down in the upper soft and highly compressible clay layer (Fig. 2). Detailed analyses on the effects of Bangkok land subsidence, induced by deep-well pumping on geo-hazard (flooding), and the ground improvement scheme, are recently reported by Shibuya et al. (2003) and Balasubramaniam et al. (2005).

Based on extensive field and laboratory studies carried out in the past by numerous researchers (see Brand and Balasubramaniam, 1976; AIT, 1981; Shibuya et al., 2003; Balasubramaniam et al., 2009) the following

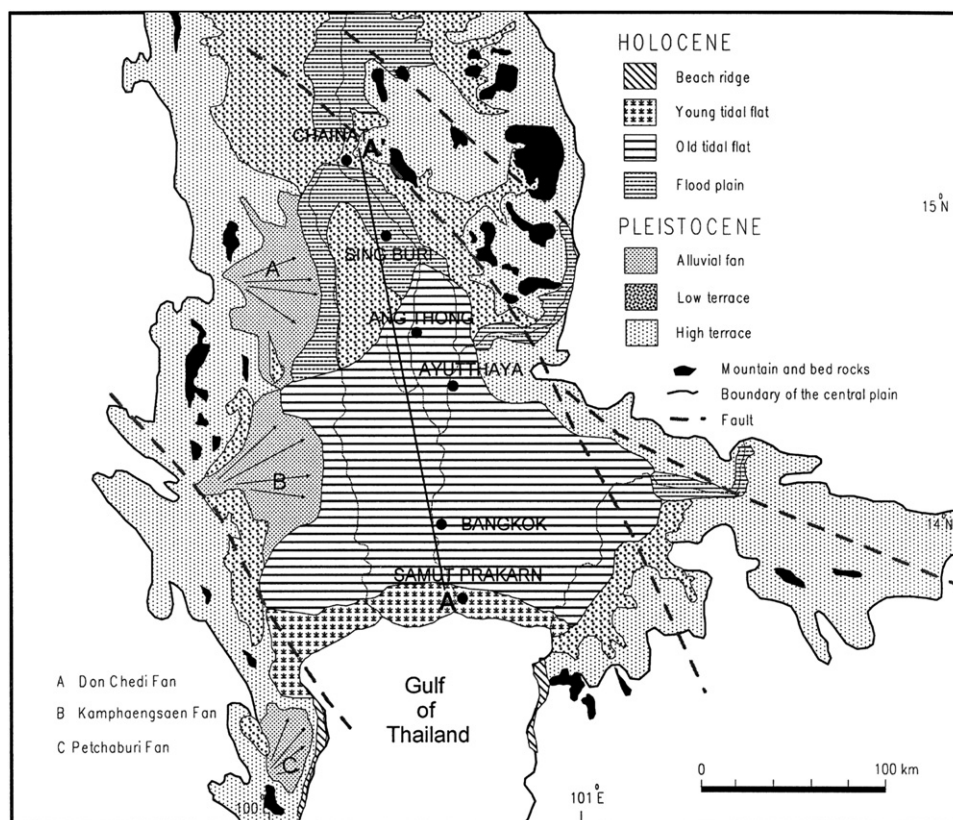


Fig. 1. Geologic map of Quaternary deposits in the Lower Central Plain of Thailand (Sinsakul, 2000).

descriptions have been proposed for the soft and stiff Bangkok clays.

(1) *Weathered Crust (WC) and Backfill*—The uppermost layer is the fill material (very loose to medium dense silty sand) and weathered crust (medium to stiff silty clay), which is light to yellowish grey in colour. The average thickness is about 2–5 m in most areas, with the SPT N-value ranging from 2 to 21. The water content is 10–35%. The ground-water table is found to be within this layer.

- (2) *Very Soft to Soft Bangkok Clay (BSC: Bangkok Soft Clay)*—The very soft to soft Bangkok clay layer located at depths of 3 and 12 m; medium grey to dark grey in colour; undrained shear strength 10–30 kN/m²; natural water content of 60–105%.
- (3) *Medium Stiff to Very Stiff Clay (FSC: First Stiff Clay)*—Dark grey to brownish grey; medium stiff to very stiff clay; thickness 15–35 m; undrained shear strength 26–160 kN/m²; natural water content of 15–60%.

The index properties for Weathered, Soft and Stiff Bangkok clays are summarised in Table 1.

3. Soil models and associated parameters

The early experimental work on the stress–strain behaviour of Bangkok subsoils was particularly aimed to validate the critical state theories as established at the Cambridge University (see Roscoe and Burland, 1968). Particular emphasis was made in verifying the Critical State Models for application in finite element analysis using CRISP computer programme. In this programme, the soil parameters are directly evaluated from triaxial compression tests and the basic parameters include only the compression index, the swell index and the angle of internal friction. It was used extensively in the study of embankments on soft soils with and without ground improvement. The PLAXIS software became available subsequently and was more user friendly. Constitutive models used in PLAXIS are in line with five categories as presented by Schweiger (2009):

- (1) *Linear or non-linear elastic models*—Soil behaviour is said to be elastic, with one stiffness parameter used. However, the results from this model are very far from real soil behaviour and, therefore, it should not be adopted in practice.
- (2) *Elastic-perfectly plastic models*—The elastic-perfectly plastic (i.e. Mohr–Coulomb) model, is relatively simple, and is

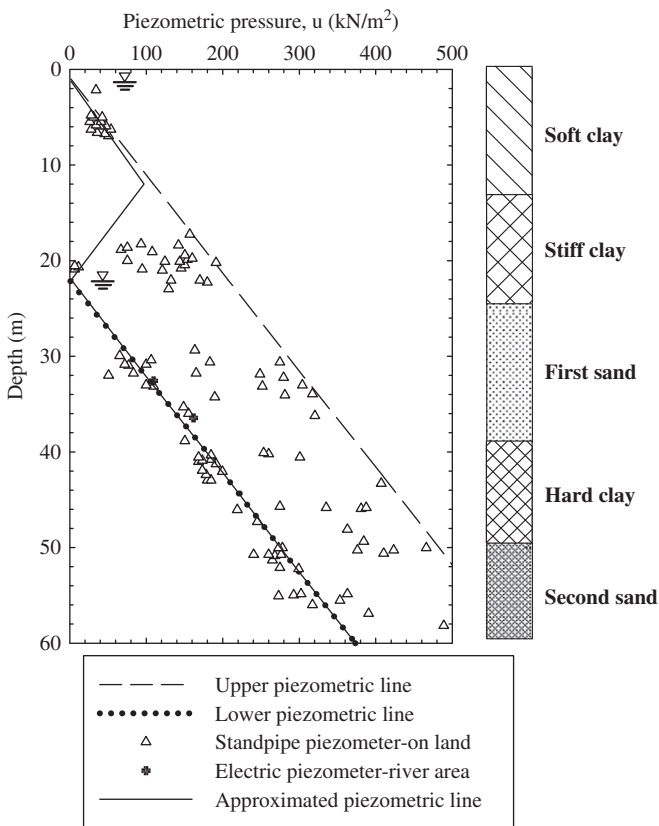


Fig. 2. Piezometric pressure in Bangkok subsoils.

Table 1
Index properties of Bangkok clays.

| Properties | Weathered clay | Soft clay | Stiff clay |
|--------------------------------------|----------------|---------------|---------------|
| Natural water content (%) | 133 ± 5 | 122–130 | 20–24 |
| Natural voids ratio | 3.86 ± 0.15 | 3.11–3.64 | 1.10–1.30 |
| Grain size distribution | | | |
| Sand (%) | 7.5 | 4.0 | 23 |
| Silt (%) | 23.5 | 31.7 | 43 |
| Clay (%) | 69 | 64.3 | 34 |
| Specific gravity | 2.73 | 2.75 | 2.74 |
| Liquid limit (%) | 123 ± 2 | 118 ± 1 | 46 ± 2 |
| Plastic limit (%) | 41 ± 2 | 43 ± 0.5 | 19 ± 2 |
| Dry unit weight (kN/m ³) | 15.8 ± 0.3 | 16.5 | 15.5–16.5 |
| Consistency | Soft | Soft | Stiff |
| Colour | Dark grey | Greenish grey | Greenish grey |
| Degree of saturation (%) | 95 ± 2 | 98 ± 2 | 94–100 |

considered the most widely used model among practising engineers. The elastic-perfectly plastic model seems to be sufficient for some areas of geotechnical problems, especially when being used by experienced engineers. However, a great care must be taken because the stress path predicted by this model can be misleading and results in an over-prediction of soil strength in the case of soft clays.

- (3) *Isotropic hardening single surface plasticity models*—The isotropic hardening single surface plasticity model such as the Modified Cam Clay (MCC) model is the first step to modelling real soil behaviour. The MCC Model introduced an elliptic yield surface which separates the elastic behaviour from the plastic behaviour. The application of this model has been widely accepted, especially for cases of embankments on soft clay. Where there is an unloading problem, such as an excavation, the soil stress path remains generally inside the yield surface. Thus, the predicted deformations are governed by the elastic behaviour.
- (4) *Isotropic hardening double surface plasticity models*—The isotropic hardening double surface plasticity model for example the Hardening Soil Model (HSM) (Schanz et al., 1999) gives more realistic displacement patterns for the working load conditions, especially in the case of an excavation. The predicted ground movement patterns induced by tunnelling are realistic and have no influence on the finite element boundary conditions (Schweiger, 2009).
- (5) *Kinematic hardening multi-surface plasticity models*—The kinematic hardening multi-surface plasticity models are generally able to capture more complex soil behaviour, including softening, small strain, anisotropy, and structured soils. Examples of soil models in this category are the Kinematic Hardening Model or Bubble Model (Al-Tabbaa and Wood, 1989; Wood, 1995), and the Three-Surface Kinematic Hardening (3-SKH) Model (Atkinson and Stallebrass, 1991). Other, more complex, soil models, such as the MIT-E3 Model (Whittle and Kavvas, 1994), use different assumptions, for example, non-linear behaviour in recoverable state and non-associated flow rule. These models require large numbers of, and more

complicated, input parameters. They are not yet available in commercial finite element software.

This paper concentrates on the use of the Hardening Soil Model (HSM) in the PLAXIS finite element software, which can be briefly explained in the following section

3.1. Hardening Soil Model in PLAXIS

Initially, the Hardening Soil Model (HSM) was introduced in the PLAXIS programme as an extension of the Mohr–Coulomb Model (Nordal, 1999). Then, in PLAXIS Version 7, an additional cap was added to the model to allow for the pre-consolidation pressure to be taken into account. Indeed, the HSM has been developed under the framework of the theory of plasticity. In the model, the total strains are calculated using a stress-dependent stiffness, which is different for both loading and unloading/reloading. The hardening is assumed to be isotropic, depending on the plastic shear and volumetric strains. A non-associated flow rule is adopted when related to frictional hardening and an associated flow rule is assumed for the cap hardening.

Schanz et al. (1999) and Brinkgreve (2002) explained in detail, the formulation and verification of the Hardening Soil Model. The essential backgrounds of the model are summarised in this section. A total of 10 input parameters are required in the Hardening Soil Model, as tabulated in Table 2.

Unlike the Mohr–Coulomb Model, the stress–strain relationship, due to the primary loading, is assumed to be a hyperbolic curve in the HSM. The hyperbolic function, as given by Kondner (1963), for the drained triaxial test can be formulated as

$$\varepsilon_1 = \frac{q_a}{2E_{50}} \frac{q}{q_a - q}, \quad \text{for } q < q_f \quad (1)$$

where ε_1 is the axial strain, and q is the deviatoric stress. The ultimate deviatoric stress (q_f) is defined as

$$q_f = \frac{6 \sin \phi'}{3 - \sin \phi'} (\sigma'_3 + c' \cot \phi'), \quad (2)$$

Table 2
Hardening soil model input parameters.

| Parameter | Description | Parameter evaluation |
|-----------------|---|--|
| ϕ' | Internal friction angle | Slope of failure line from MC failure criterion |
| c' | Cohesion | y-intercept of failure line from MC failure criterion |
| R_f | Failure ratio | $(\sigma_1 - \sigma_3) / (\sigma_1 - \sigma_3)_{ult}$ |
| ψ | Dilatancy angle | Function of ε_a and ε_v |
| E_{50}^{ref} | Reference secant stiffness from drained triaxial test | y-intercept in $\log(\sigma_3/p^{ref}) - \log(E_{50})$ space |
| E_{oed}^{ref} | Reference tangent stiffness for oedometer primary loading | y-intercept in $\log(\sigma_1/p^{ref}) - \log(E_{oed})$ space |
| E_{ur}^{ref} | Reference unloading/reloading stiffness | y-intercept in $\log(\sigma_3/p^{ref}) - \log(E_{ur})$ space |
| m | Exponential power | Slope of trend-line in $\log(\sigma_3/p^{ref}) - \log(E_{50})$ space |
| ν_{ur} | Unloading/reloading Poisson's ratio | 0.2 (default setting) |
| K_o^{nc} | Coefficient of earth pressure at rest (NC state) | 1-sin ϕ' (default setting) |

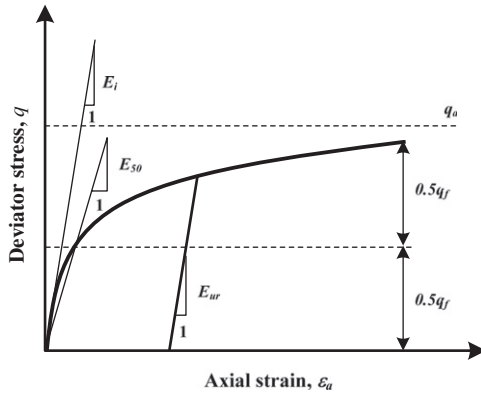


Fig. 3. Hyperbolic stress–strain relationship in primary loading for a standard drained triaxial test (Schanz et al., 1999).

and the quantity (q_a) is

$$q_a = \frac{q_f}{R_f} \quad (3)$$

where q_f is the ultimate deviatoric stress at failure, which is derived from the Mohr–Coulomb failure criterion involving the strength parameters c' and ϕ' . The q_a is the asymptotic value of the shear strength. The R_f is the failure ratio. If $q_f = q_a$ ($R_f = 1$), the failure criterion is satisfied and perfectly plastic yielding occurs. The failure ratio (R_f) in PLAXIS is given as 0.9 for the standard default value. Fig. 3 shows the hyperbolic relationship of stress and strain in primary loading.

The stress–strain behaviour for primary loading is highly non-linear. The parameter E_{50} is a confining stress dependent stiffness modulus for primary loading. E_{50} is used instead of the initial modulus E_0 for small strain which, as a tangent modulus, is more difficult to determine experimentally, and is given as

$$E_{50} = E_{50}^{ref} \left(\frac{c' \cos \phi' - \sigma'_3 \sin \phi'}{c' \cos \phi' + p^{ref} \sin \phi'} \right)^m \quad (4)$$

where E_{50}^{ref} is a reference stiffness modulus corresponding to the reference stress p^{ref} . In PLAXIS, a default setting $p^{ref} = 100 \text{ kN/m}^2$, is used. The actual stiffness depends on the minor effective principal stress σ'_3 , which is the effective confining pressure in a triaxial test. Note that in PLAXIS, σ'_3 is negative in compression. The amount of stress dependency is given by the power m . In order to simulate a logarithmic stress dependency, as observed for soft clay, m should be taken as 1. Soos von (2001) reported a range of m values from 0.5 to 1 in different soil types with the values of 0.9–1 for the clay soils.

The stress dependent stiffness modulus for unloading and reloading stress paths is calculated as

$$E_{ur} = E_{ur}^{ref} \left(\frac{c' \cos \phi' - \sigma'_3 \sin \phi'}{c' \cos \phi' + p^{ref} \sin \phi'} \right)^m \quad (5)$$

where E_{ur}^{ref} is the reference modulus for unloading and reloading, which corresponds to the reference pressure p^{ref}

($p^{ref} = 100 \text{ kN/m}^2$ by default setting). For a practical case, PLAXIS gives the default setting of E_{ur}^{ref} equal to $3E_{50}^{ref}$.

The shear hardening yield function (f_s) in the HSM is given as

$$f_s = \bar{f} - \gamma^p \quad (6)$$

$$\bar{f} = \frac{q_a}{E_{50}} \left\{ \frac{(\sigma'_1 - \sigma'_3)}{q_a - (\sigma'_1 - \sigma'_3)} \right\} - \frac{2(\sigma'_1 - \sigma'_2)}{E_{ur}} \quad (7)$$

where σ'_1 and σ'_3 are the major and minor effective principal stresses, E_{50} is 50% secant stiffness modulus, and γ^p is the plastic shear strain, and can be approximated as

$$\gamma^p \approx \varepsilon_1^p - \varepsilon_2^p - \varepsilon_3^p = 2\varepsilon_1^p - \varepsilon_v^p \approx 2\varepsilon_1^p \quad (8)$$

where $\varepsilon_1^p, \varepsilon_2^p$, and ε_3^p are the plastic strains, and ε_v^p is the plastic volumetric strain.

From the formulations of the shear hardening yield function (Eqs. (6)–(8)), it can be seen that the triaxial moduli (E_{50}^{ref} and E_{ur}^{ref}) are parameters that control the shear hardening yield surfaces. In addition to the shear hardening yield surfaces, the cap yield surfaces are also used in the HSM. These cap yield surfaces are related to the plastic volumetric strain measured in the isotropic compression condition. Fig. 4 shows the shear hardening and the cap yield surfaces in the HSM for soil with no cohesion ($c' = 0$).

Another input parameter, the reference oedometer modulus (E_{oed}^{ref}), is used to control the magnitude of the plastic strains that originate from the yield cap (ε_v^{pc}). In a similar manner to the triaxial moduli, the oedometer modulus (E_{oed}) obeys the stress dependency law:

$$E_{oed} = E_{oed}^{ref} \left(\frac{c' \cos \phi' - \sigma'_1 \sin \phi'}{c' \cos \phi' + p^{ref} \sin \phi'} \right)^m \quad (9)$$

The definition of the cap yield surface can be given as

$$f^c = \frac{\tilde{q}^2}{\alpha^2} + p^2 - p_p^2 \quad (10)$$

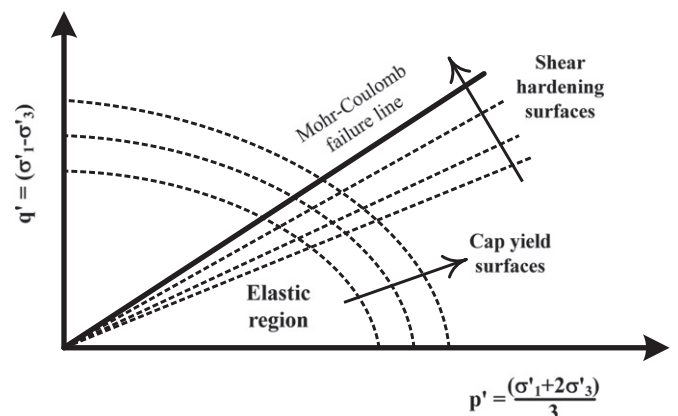


Fig. 4. Shear hardening and cap yield surfaces in the Hardening Soil Model (Schanz et al., 1999).

where, α is an auxiliary model parameter related to K_o^{nc} (see below). The parameters p and \tilde{q} are expressed as

$$p = \frac{-(\sigma_1 + \sigma_2 + \sigma_3)}{3} \tag{11}$$

$$\tilde{q}^2 = \sigma_1 + (\delta - 1)\sigma_2 - \sigma_3 \tag{12}$$

where

$$\delta = \frac{(3 + \sin \phi')}{(3 - \sin \phi')} \tag{13}$$

\tilde{q} is the special stress measure for deviatoric stresses. In the case of the triaxial compression \tilde{q} reduces to $\tilde{q} = -\delta(\sigma_1 - \sigma_3)$.

The magnitude of the yield cap is determined by the isotropic pre-consolidation stress p_p . Importantly, the hardening law, which relates the pre-consolidation pressure (p_p) to the volumetric cap-strain (ϵ_v^{pc}), can be expressed as

$$\epsilon_v^{pc} = \frac{\beta}{1-m} \left(\frac{p_p}{p^{ref}} \right)^{1-m} \tag{14}$$

where ϵ_v^{pc} is the volumetric cap strain, which represents the plastic volumetric strain in isotropic compression. In addition to the constants m and p^{ref} , which have been discussed earlier, there is another model constant β . Both α and β are cap parameters, but PLAXIS does not adopt them as input parameters. Instead, their relationships can be expressed as:

$$\alpha = K_o^{nc} \quad (\text{by default } K_o^{nc} = 1 - \sin \phi') \tag{15}$$

$$\beta = E_{oed}^{ref} \quad (\text{by default } E_{oed}^{ref} = E_{50}^{ref}) \tag{16}$$

Such that K_o^{nc} and E_{oed}^{ref} can be used as input parameters that determine the magnitude of α and β , respectively. Fig. 5 shows the ellipse shape cap surface in the p - q plane.

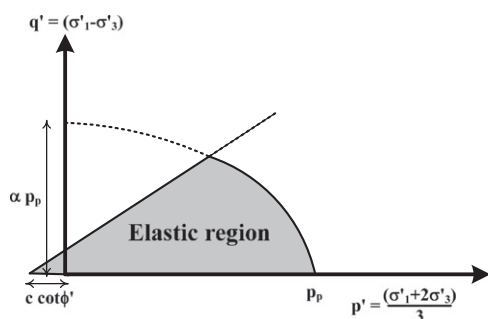


Fig. 5. Yield surface of the Hardening Soil Model in q - p' plane (Schanz et al., 1999).

4. Evaluation of strength and stiffness parameters for soft and stiff Bangkok clays

4.1. Details of soil sampling and testing procedures

All the test results analysed in this study were determined for undisturbed samples taken at the appropriate depths for soft clay, medium stiff clay and stiff clay. The 25.4 mm diameter and long thin walled sample tubes were used for soft and medium stiff clays are used for triaxial tests in Weathered, soft and medium stiff clays. For the stiff clay, and the Oedometer tests 625 mm samples were taken and used. After extruding, the samples for soft, and medium stiff clay were cut into 100 mm high sections, covered with wax and paraffin, and stored in the humidity controlled moist room. These were used for the triaxial tests. For the Oedometer tests, the samples were extruded from the tubes and used directly.

4.1.1. Oedometer tests

Numerous Oedometer tests were carried out on undisturbed samples of soft, medium stiff and stiff Bangkok clays (Nanegrungsung, 1976; Tonyagate, 1978; Kerdsuwan, 1984; Koslanant, 1997). In addition there are reports on the Bangkok subsidence studies, Bangkok Airport Project and MRTA works. The testing procedures adopted were based on extensive research work carried out at the Asian Institute of Technology by the fourth author on Oedometer consolidation with standard lever arm consolidometer, Bishop type hydraulic cell and Rowe cells for samples of Bangkok clays collected from various depths up to 90 m. The data analysed in this paper were obtained for 625 mm samples taken at the relevant depths. The Lever-arm consolidometer used for the testing consisted of one piece rigid casting 625 mm diameter and 19.0 mm thick. The sample was placed in rigid walled cell between upper and lower porous stones for vertical drainage. A load increment ratio of one was used in all the tests. Depending on the type of Bangkok clay tested, the load increments were kept for at least 24 h or until the pore pressure was fully dissipated.

4.1.2. Triaxial tests

For the triaxial testing, each sample was taken out from the moist room, paraffin and wax carefully removed and trimmed down to the required size. Two porous stones were placed one at each end of the sample. Also, Whatman no. 40 filter paper side drains were placed along the circumference. The sample was then enclosed within two rubber membranes which were separated by a thin coating of silicone grease. The upper and lower ends of the rubber membrane were sealed against the top cap and the pedestal respectively by hard Gabo “O” ring seals. The chamber surrounding the sample was then filled with silicone oil. For all the tests, the samples were consolidated isotropically to various consolidation pressures against an elevated pore pressure to endure saturation. A back pressure of

207 kN/m² was applied to all the specimens, which has been found sufficient to remove all the air. The volume change of the sample was measured at various intervals until all the excess pore pressure was dissipated. Depending on the consolidation pressure, the time required for full dissipation of pore pressures varied from 2 to 5 day.

In this paper, the results of several series of compression and extension tests carried out on Weathered Clay, Soft Clay and Stiff Clay are analysed. Test specimens were approximately 72 mm in height and 36 mm in diameter. Several series of isotropically consolidated drained and undrained compression (CID, CIU) and extension (CIUE, CIDE) tests carried out at the Asian Institute of Technology were re-analysed in this study. Most of the CID, CIU, CIDE and CIUE tests were carried out under strain controlled conditions (Ahmed, 1976; Hassan, 1976; Balasubramaniam, and Uddin, 1977; Li1975; Hwang, 1975). In addition, some load controlled CID and CIU tests were also considered (Chaudhry, 1975).

In order to eliminate the effect of strain rate, a constant rate of strain was used for each type of strain controlled test. However, the particular strain rate value for each triaxial test was chosen taken into account time required for the equalisation of pore water pressure within the sample. Following the work of Henkel and Gibson (1954), the following shearing rates were chosen:

- 0.0018 in./min for CIU and CIUE tests on Weathered Clay,
- 0.000048 in./min for CID and CIDE tests on Weathered and Soft Clay,

- 0.00048 in./min for CIU and CIUE tests on Stiff Clay.
- 0.000032 in./min for CID and CIDE tests on Stiff Clay.

The shearing in CIU and CID tests on Soft Clay was carried out under stress controlled conditions by addition of series of dead load increments to the ram through a hanger. In this series of tests, two load increment durations (i.e. 1 h and 1 day) were adopted. However, the behaviours of the specimens sheared under both durations were practically identical. The size of a few initial load increments was varied between 10–12% and 20–25% of the failure load. Subsequently, these values were reduced in stages to 2–5% of the failure load at around the peak stress state.

It should also be pointed out that all the triaxial test data were corrected for strength of rubber membranes and filter paper drains. For more details of triaxial testing procedures, see Balasubramaniam and Uddin (1977), Balasubramaniam and Chaudhry (1978), and Balasubramaniam et al. (1978).

4.2. Mohr–Coulomb strength parameters

Table 3 presents a summary of the Mohr–Coulomb strength parameters of the Bangkok subsoils (i.e. weathered clay, soft clay, stiff clay and hard clay) obtained from consolidated isotropically drained and undrained triaxial compression (CID and CIU) and extension (CIDE and CIUE) tests reported in

Table 3
Summary of Mohr–Coulomb strength parameter of Bangkok subsoils.

| Reference | Location | Depth (m) | Test type | ϕ' (deg) | c' (kN/m ²) |
|---|---------------|-----------|-------------------|------------------|------------------------------|
| <i>Weathered clay</i> | | | | | |
| Balasubramaniam and Uddin (1977) | Nong Ngoo Hao | 2.5–3.0 | CIUE _U | 28.9 | 0 |
| Balasubramaniam et al. (1978) | Nong Ngoo Hao | 2.5–3.0 | CIU | 22.2 | 0 |
| | | | CID | 23.5 | 0 |
| | | | CIUE _U | 29 | 0 |
| <i>Soft clay</i> | | | | | |
| Balasubramaniam and Chaudhry (1978) | Nong Ngoo Hao | 5.5–6.0 | CIU | 26 | 0 |
| | | | CID | 21.7 | 0 |
| Balasubramaniam et al. (1978) | Nong Ngoo Hao | 5.5–6.0 | CIU | 24 | 38 |
| | | | CID | 23.5 | 0 |
| | | | CIDP | 23.7 | 0 |
| | | | CIUE ^L | 26 | 0 |
| | | | CIUE ^U | 21.1 | 58.7 |
| | | | CIDE ^L | 26.2 | 0 |
| | | | CIDE ^U | 23.5 | 31.8 |
| <i>Stiff clay</i> | | | | | |
| Ahmed (1976), Balasubramaniam et al. (1978) | Nong Ngoo Hao | 16.0–16.6 | CID | 26 | 30 |
| | | | CIUE ^L | 18 | 54 |
| | | | CIUE ^U | 25 | 54 |
| | | | CIDE ^U | 16.6 | 11 |
| Hassan (1976) | Nong Ngoo Hao | 17.0–18.0 | CIU | 28.1 | 11.4 |
| | | | CID | 26.3 | 32.8 |

the literature. The notations for the triaxial tests identified in Table 3 are explained. It can be seen that the differences in the applied stress path have the most significant effect on the Mohr–Coulomb strength parameters. Initial conditions at the consolidation state (i.e. isotropic or anisotropic), as well as the drainage conditions during shear (i.e. drained or undrained), also have an effect on the strength parameters, but to a lesser magnitude. Therefore, it needs to be emphasised that the strength parameters should be carefully selected according to the applied stress path, resulting from the construction sequences.

4.3. Oedometer test data

The Oedometer tests were conducted on soft clay at 6–8 m depths; medium stiff clay at 12–14 m depths; and stiff clay at 15.5–18 m depths. The resulting reference oedometer moduli ($E_{oed}^{ref}, E_{ur,oed}^{ref}$), the modulus power (m), the critical state consolidation parameters (λ^*, κ^*) are presented in Table 4. The reference moduli E_{oed}^{ref} and $E_{ur,oed}^{ref}$ are found by plotting normalised E_{oed} and $E_{ur,oed}$ versus normalised σ_1' in double log scale plots, as shown in Fig. 6. In this plot, the reference loading and unloading/reloading

constrained moduli ($E_{oed}^{ref}, E_{ur,oed}^{ref}$) can be found from the y-intercept of their linear trend lines; while the modulus power (m) is the slope of the same lines. Fig. 6 shows the average values of $E_{oed}^{ref}, E_{ur,oed}^{ref}$ and their modulus power (m) for soft clay layer (6–8 m), medium clay (12–14 m), and stiff clay (15.5–18 m), respectively.

The averaged values of $E_{oed}^{ref}, E_{ur,oed}^{ref}$ and m parameters required as input stiffness parameters of the HSM for each subsoil layer are summarised in Table 5. The averaged values of E_{oed}^{ref} are in the order of 926, 1650, and 4689 kN/m² for soft, medium, and stiff clays, respectively. For $E_{ur,oed}^{ref}$, these average values are 5813, 5394, and 9618 kN/m², respectively. The values of the power (m) are close to unity for E_{oed}^{ref} in soft clay and for $E_{ur,oed}^{ref}$ in all layers. This finding is in agreement with the power m of 1 for normally consolidated clay (Janbu, 1963). The values of power m for E_{oed}^{ref} in medium and stiff clays are, however, reducing to 0.6. The ratios of $E_{ur,oed}^{ref}/E_{oed}^{ref}$ in the soft clay layer generally range from 2 to 4. These average values are also summarised in Table 4.

4.4. Triaxial tests data

4.4.1. Soft Bangkok clay

Two series of isotropically consolidated triaxial compression tests, CIU and CID, conducted by Chaudhry (1975) on soft and stiff Bangkok clay, were analysed in this study. The soil samples were taken from a depth of 6.0 m below the ground surface. The confining pressures, σ_3' used for both CIU and CID series were 138, 207, 276, 345 and 414 kN/m² for tests S1–S5, respectively. The angle of the internal friction (ϕ') obtained from the CIU and CID tests were 27° and 23.6°; whereas, the cohesion (c') was zero for

Table 4
Consolidation parameters results from Oedometer tests.

| Test | Loading | | Un/re-loading | | $E_{ur,oed}^{ref}/E_{oed}^{ref}$ | λ^* | κ^* |
|------------------------------------|--------------------------------------|-----|---|-----|----------------------------------|-------------|------------|
| | E_{oed}^{ref} (kN/m ²) | m | $E_{ur,oed}^{ref}$ (kN/m ²) | m | | | |
| <i>Soft clay (6–8 m)</i> | | | | | | | |
| 1 | 901 | 0.9 | 7679 | 1.1 | 8.5 | 0.115 | 0.009 |
| 2 | 1068 | 1.0 | 4310 | 1.5 | 4.0 | 0.094 | 0.008 |
| 3 | 858 | 0.9 | 7546 | 1.1 | 8.8 | 0.122 | 0.010 |
| 4 | 1105 | 0.7 | 4532 | 1.2 | 4.1 | 0.111 | 0.013 |
| <i>Medium stiff clay (12–14 m)</i> | | | | | | | |
| 5 | 2282 | 0.6 | 8989 | 1.2 | 3.9 | 0.073 | 0.006 |
| 6 | 1429 | 0.6 | 2903 | 0.6 | 2.0 | 0.110 | 0.023 |
| 7 | 1749 | 0.5 | 7663 | 1.0 | 4.4 | 0.099 | 0.012 |
| 8 | 1288 | 0.6 | 4126 | 1.2 | 3.2 | 0.113 | 0.015 |
| <i>Stiff clay (15.5–18 m)</i> | | | | | | | |
| 9 | 5548 | 0.6 | 8670 | 1.1 | 1.6 | 0.033 | 0.009 |
| 10 | 5187 | 0.7 | 12,451 | 1.0 | 2.4 | 0.032 | 0.007 |
| 11 | 3736 | 0.6 | 8241 | 1.0 | 2.2 | 0.049 | 0.012 |

Table 5
Summary of averaged $E_{oed}^{ref}, E_{ur,oed}^{ref}$ and m .

| Subsoils | Depth(m) | Loading | | Un/Re-loading | |
|-------------------|----------|--------------------------------------|-----|---|-----|
| | | E_{oed}^{ref} (kN/m ²) | m | $E_{ur,oed}^{ref}$ (kN/m ²) | m |
| Soft clay | 6–8 | 926 | 0.9 | 5813 | 1.2 |
| Medium stiff clay | 12–14 | 1650 | 0.6 | 5394 | 1.0 |
| Stiff clay | 15.5–18 | 4689 | 0.6 | 9618 | 1.0 |

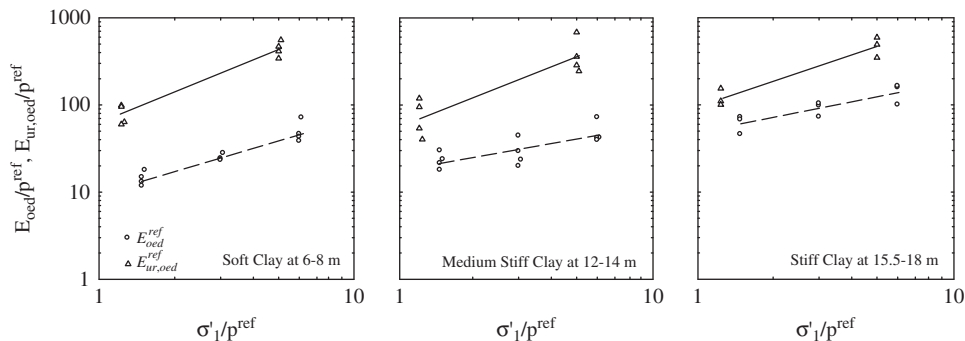


Fig. 6. Oedometer Moduli versus consolidation pressure of Bangkok Soils.

both series. The drained strength parameters are summarised in Table 6.

The results of the CIU triaxial tests carried out on the soft clay are plotted in Fig. 7. The (q, ϵ_a) and (u, ϵ_a) relationships are shown in Fig. 7(a) and (b), respectively. The deviator stress and excess pore pressures versus the axial strain relationships show typical normally to lightly overconsolidated clay behaviour, where the deviator stress and excess pore pressure reaches their ultimate values at a relatively large strain. Moreover, all the excess pore pressure plots were located in the positive range.

The results obtained from the CID triaxial tests for the soft clay are shown in Fig. 8, with the relationships of (q, ϵ_a) and (ϵ_v, ϵ_a) plotted in Fig. 8(a) and (b), respectively. It can be seen that, during the deviator stress applied, the volume of the soil specimen gradually reduces. The volumetric and axial strain curves of all the tests seem to

Table 6
Stiffness and strength parameters from CID and CIU tests for Bangkok clays.

| Parameters | CID | CIU |
|---|---------|---------|
| <i>Soft Bangkok clay</i> | | |
| Confining pressure (kN/m ²) | 138–414 | 138–414 |
| Initial $E_i^{ref}, E_{u,i}^{ref}$ (kN/m ²) | 1343 | 7690 |
| m | 1.0 | 1.2 |
| 50% $E_{50}^{ref}, E_{u,50}^{ref}$ (kN/m ²) | 690 | 4831 |
| m | 1.1 | 1.0 |
| R_f | 0.72 | 0.94 |
| ϕ' | 23.6 | 27.0 |
| c' (kN/m ²) | 0 | 0 |
| <i>Stiff Bangkok clay</i> | | |
| Confining pressure (kN/m ²) | 34–552 | 17–620 |
| Initial $E_i^{ref}, E_{u,i}^{ref}$ (kN/m ²) | 29,676 | 30,109 |
| m | 0.52 | 0.46 |
| 50% $E_{50}^{ref}, E_{u,50}^{ref}$ (kN/m ²) | 14,398 | 11,104 |
| m | 0.48 | 0.53 |
| R_f | 0.89 | 0.88 |
| ϕ' | 26.3 | 28.1 |
| c' (kN/m ²) | 32.8 | 11.4 |

coincide up to 10% axial strain, after that they tend to divert slightly.

An example of the reference moduli at 50% of strength ($E_{50}^{ref}, E_{u,50}^{ref}$) and power m determined from the CIU and CID tests using double log scale plots is given in Fig 9. These values are also summarised in Table 6 together with the reference initial modulus ($E_i^{ref}, E_{u,i}^{ref}$), the reference moduli at 50% of strength ($E_{50}^{ref}, E_{u,50}^{ref}$), and the failure ratio (R_f) resulting from CID tests as well as the shear strength parameters (c', ϕ') for Soft Bangkok Clay.

4.4.2. Stiff Bangkok clay

The two series of isotropically consolidated triaxial compression tests, CIU and CID, conducted by Hassan (1976) on stiff Bangkok clay, are re-interpreted in this study. The undisturbed soils samples were collected from a depth of 17.4–18 m below the ground surface. The pre-shear consolidation pressures ranged from 17 to 620 kN/m² and 34–552 kN/m², for the CIU and CID series, respectively. The angles of the internal friction (ϕ') from the CIU and CID series were 28.1° and 26.3°; whereas, the values of cohesion (c') were 11.4 and 32.8 kN/m², respectively. The drained strength parameters are summarised in Table 6.

Fig. 10 shows the results of CIU tests on the stiff Bangkok clay. It can be seen from Fig. 10(a) that (q, ϵ_a) relationships, up to a pre-shear confining pressure of 138 kN/m² (tests CIU F1–F3), exhibit no strain softening. At a level of confining pressure from 207 to 414 kN/m² (tests CIU F4–F7), these clay samples behaved as heavily overconsolidated clay showing a clear peak deviator stress at a low axial strain, followed by a strain softening. Beyond the confining pressure of 552 kN/m² (tests CIU F8 and F9), these samples behaved as lightly overconsolidated clay.

The relationships between the excess pore pressure and the axial strain are shown in Fig. 10(b). For all clay samples (CIU F1–F9), the excess pore pressure increases as the deviator stress increases, until the peak values are reached at 1–4% axial strain, depending on the confining pressure. The peak excess pore pressure seems to be

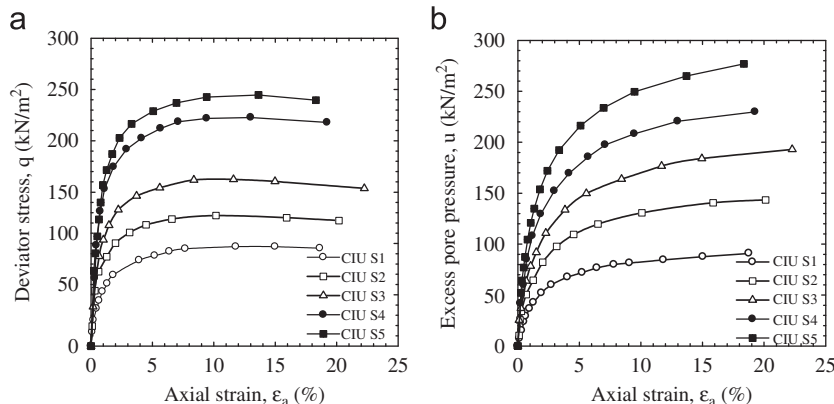


Fig. 7. Results of CIU triaxial tests on soft Bangkok clay. (a) Deviator stress versus axial strain and (b) Pore pressure versus axial strain.

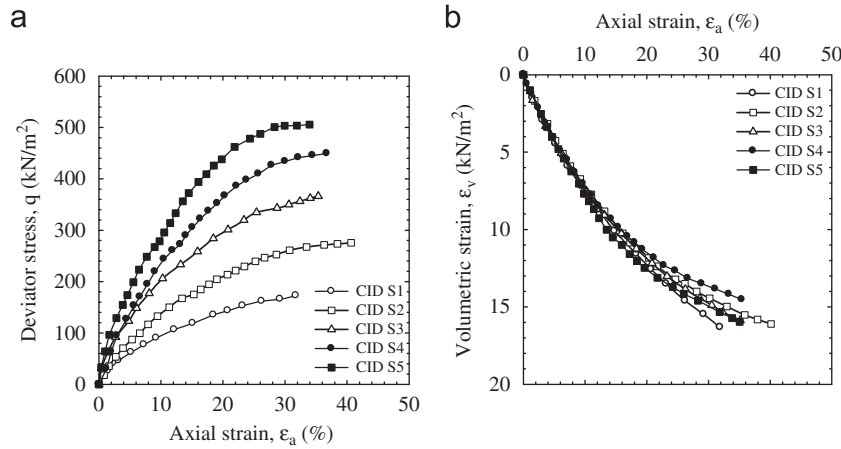


Fig. 8. Results of CID triaxial tests on soft Bangkok clay. (a) Deviator stress versus axial strain and (b) Volumetric strain versus axial strain.

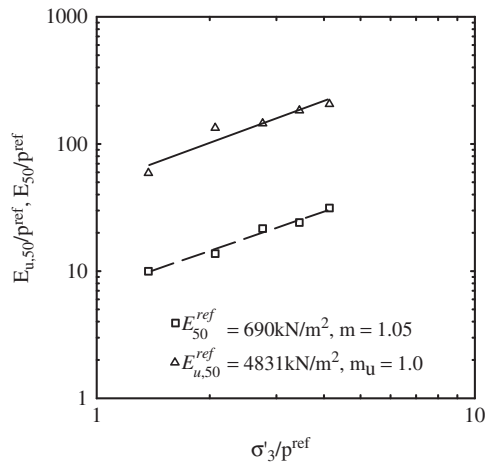


Fig. 9. Variations of E_{50} and $E_{u,50}$ with confining pressure for Soft Bangkok Clay.

reached at a higher axial strain as the confining pressure increases. As the sample was further sheared, the excess pore pressure gradually reduced to the minimum value, at approximately 12% axial strain. Only the first three samples (tests CIU F1–F3) reached negative excess pore pressures.

The results of CID triaxial tests carried out on the stiff Bangkok clay are shown in Fig. 11. The deviator stress versus the axial strain relationships of the stiff clay are shown in Fig. 11(a). The pre-shear confining pressures of 34, 103, 414 and 552 kN/m² were applied. None of the stiff clay samples demonstrated a well defined peak. However, samples CID F1–F3 (with confining pressure of 34, 103 and 414 kN/m²) illustrate some degree of strain softening after the peak deviator stresses are reached at axial strain levels of 3–5%. The plots of the volumetric versus the axial strain are given in Fig. 11(b). The specimens with a confining pressure of 34 and 103 kN/m² (tests CID F1 and 2) start to dilate at about 1.2 and 3.5% axial strain. The specimen at 414 kN/m² confining pressure consolidates up to an axial strain level of 8%.

After that, the volumetric strain seems to be constant with an increase in axial strain. The last specimen with a confining pressure of 552 kN/m² consolidates up to 7% of the axial strain, and then it tends to dilate.

An example of the reference moduli at 50% of strength ($E_{50}^{ref}, E_{u,50}^{ref}$) and power m , determined from CIU and CID tests in the double log scale plots, is presented in Fig. 12. The values of E_{50}^{ref} and $E_{u,50}^{ref}$ together with the deformation moduli and the failure ratios resulting from the CIU and CID series are also summarised in Table 6. It can be observed from Table 6 that the failure ratio (R_f) falls in a narrow range with an average value of 0.88. The power m for both the initial and the 50% moduli are approximately 0.5.

5. Finite element modelling and soil parameters calibration

In this section, the triaxial tests are modelled using simplified axisymmetric geometry. The parametric study of the Hardening Soil Model parameters, namely $E_{50}^{ref}, E_{oed}^{ref}, E_{ur}^{ref}, m, R_f, K_o^{nc}$ and v_{ur} , is conducted to evaluate the effects of each parameter on the triaxial relationships. Two series of undrained triaxial tests in soft and stiff clays were modelled. The HSM parameters were calibrated by means of curve fitting. The aim of this exercise was to find the HSM parameters suitable for undrained materials (i.e. soft and stiff Bangkok clays).

5.1. Finite element modelling

The triaxial tests were modelled in PLAXIS finite element software by means of an axisymmetric geometry of 1 m × 1 m unit dimensions as shown in Fig. 13. This unrealistically large dimension of the model did not influence the results, as the soil sample was set as a weightless material. The simplified geometry in the triaxial model represented one quarter of the soil sample. The deformations along the boundaries (line AC and CD) were kept free to allow for a smooth movement along the axes of symmetry, while the deformations

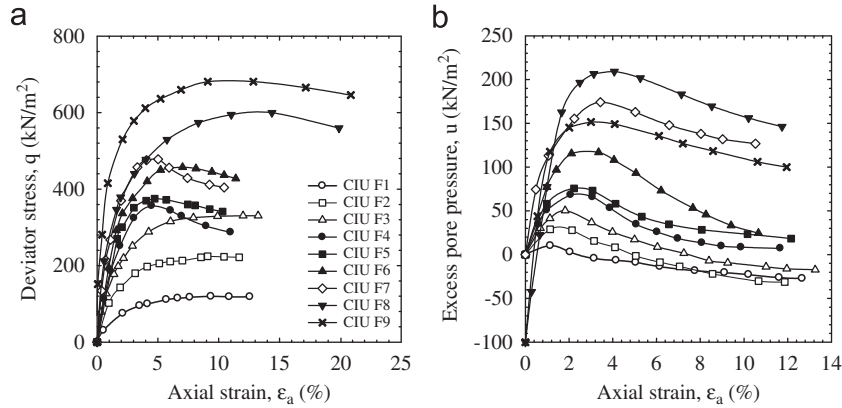


Fig. 10. Results of CIU triaxial tests on stiff Bangkok clay (a) Deviator stress versus axial strain (b) Pore pressure versus axial strain.

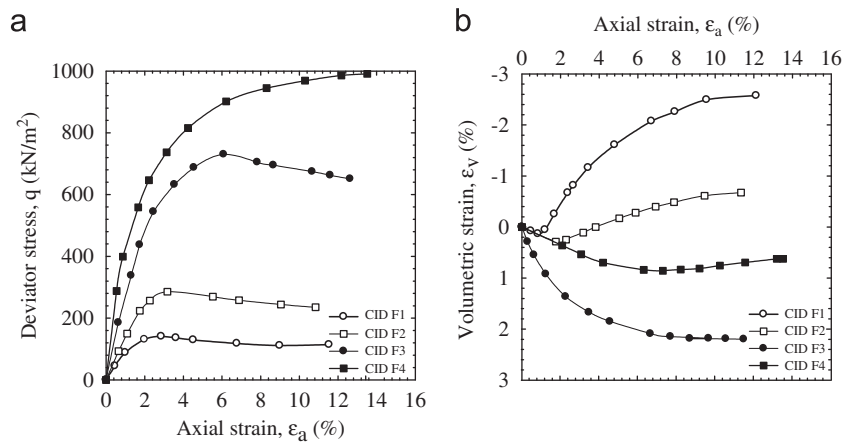


Fig. 11. Results of CID triaxial tests on stiff Bangkok clay. (a) Deviator stress versus axial strain and (b) Volumetric strain versus axial strain.

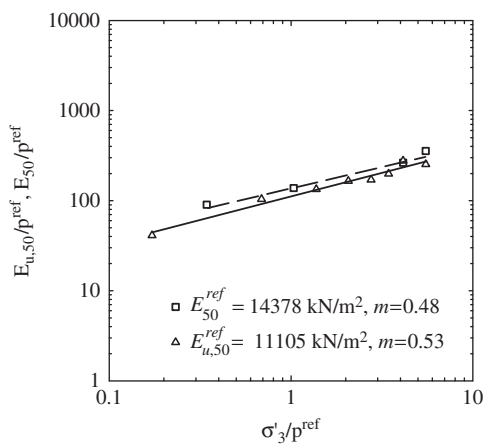


Fig. 12. Variations of E_{50} and $E_{u,50}$ with confining pressure for Stiff Bangkok Clay.

perpendicular to the boundaries were fixed. Similar to the boundary condition of the triaxial test, boundaries AB and BD were free to move. The applied deviator stress and confining pressure were simulated as a distributed load system for A and B, respectively.

In this analysis, the material type of soil clusters is set to undrained. This will allow a full development of excess pore water pressure and a flow of pore water to be neglected. Thus, the coefficient of permeability is not required in the undrained analysis. All effective stress soil parameters are utilised as presented in Tables 7 and 8. Additionally, PLAXIS automatically adds a bulk modulus of water to distinguish between effective stress and excess pore pressure. According to PLAXIS manual (Brinkgreve, 2002), an increment of effective stress ($\Delta p'$) and an increment of excess pore pressure (Δp_w) can be calculated from

$$\Delta p' = (1-B)\Delta p = K'\Delta\epsilon_v \tag{17}$$

$$\Delta p_w = B\Delta p = \frac{K_w}{n}\Delta\epsilon_v \tag{18}$$

where B is Skempton's B pore pressure parameter. K' and K_w are bulk moduli of soil skeleton and pore fluid, respectively. n is the porosity of soil and $\Delta\epsilon_v$ is an increment of volumetric strain. When, the default value

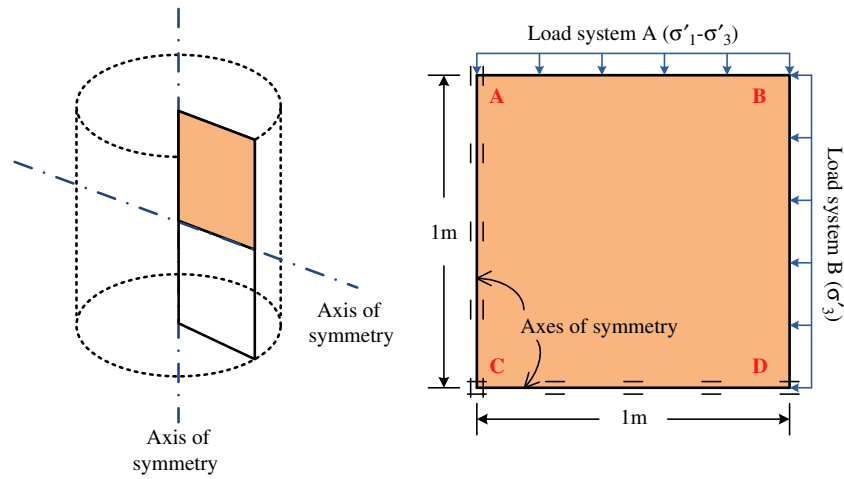


Fig. 13. Simplified geometries of triaxial test in finite element models.

Table 7
HSM input parameters based on CID and Oedometer testing results of soft Bangkok clay.

| ϕ' (deg) | ψ' (deg) | c' (kN/m ²) | E_{50}^{ref} (kN/m ²) | E_{oed}^{ref} (kN/m ²) | E_{ur}^{ref} (kN/m ²) | R_f | m | K_0^{nc} | ν_{ur} |
|---------------|---------------|---------------------------|-------------------------------------|--------------------------------------|-------------------------------------|-------|-----|------------|------------|
| 27 | 0 | 1 | 690 | 635 | 2070 | 0.9 | 1 | 0.55 | 0.2 |

Table 8
Calibrated HSM parameters for Bangkok clays.

| ϕ' (deg) | ψ' (deg) | c' (kN/m ²) | E_{50}^{ref} (kN/m ²) | E_{oed}^{ref} (kN/m ²) | E_{ur}^{ref} (kN/m ²) | R_f | m | K_0^{nc} | ν_{ur} |
|-------------------|---------------|---------------------------|-------------------------------------|--------------------------------------|-------------------------------------|-------|-----|------------|------------|
| <i>Soft clay</i> | | | | | | | | | |
| 27 | 0 | 1 | 800 | 850 | 8000 | 0.9 | 1 | 0.74 | 0.2 |
| <i>Stiff clay</i> | | | | | | | | | |
| 28 | 0 | 11.5 | 9500 | 12,000 | 30,000 | 0.9 | 1 | 0.5 | 0.2 |

of undrained Poisson’s ratio ($\nu_{ur}=0.495$) is used, a bulk modulus of water can be approximated as

$$\frac{K_w}{n} \approx 100G \tag{19}$$

A 15 noded triangular element is selected in this analysis. The cluster representing a quarter of soil sample in triaxial test is divided into soil element during the mesh generation process. The global coarseness is set to medium, thus the number of elements generated is approximately 250 elements. See Brinkgreve (2002) for more detail about the mesh generation.

5.2. HSM parameters calibration for Bangkok soft clay

In this part of the study, a series of CIU tests on the soft Bangkok clay, shown earlier in Fig. 7, was used in the Hardening Soil Model parameter calibration. However, for illustration purposes, only tests CIU S1, CIU S3 and CIU S5 ($\sigma'_3=138, 276$ and 414 kN/m²) are presented and discussed. The drained strength and stiffness parameters are needed in the undrained modelling using the HSM.

Thus, the first attempt is to use drained stiffness parameters E_{50}^{ref} from the CID test series and E_{oed}^{ref} and E_{ur}^{ref} from the oedometer test results. These parameters are listed in Table 7. Note that, the reference pressure is kept as 100 kN/m² throughout the study.

The results shown in Fig. 14 reveal poor agreements among all the stress–strain and stress path relationships. In fact, with the input parameters from Table 7, the undrained shear strengths, calculated from PLAXIS, vastly overestimated the values from the CIU test series for the entire range of confining pressures. There are two possible reasons for this outcome. Firstly, the assumption of adding bulk modulus of water, as used by the HSM in PLAXIS, to convert the drained to the undrained modulus may not be appropriate (see Surarak, 2010). Secondly, the drained moduli from CID test series (see Table 3) may not be a representative set of the Bangkok soft clay. To overcome this problem, the input parameters were adjusted in order to obtain suitable drained parameters to give the best fit results the undrained stress–strain and stress path relationships.

These best fit input parameters are shown in Table 8, while the resulting stress–strain and stress path relationships are

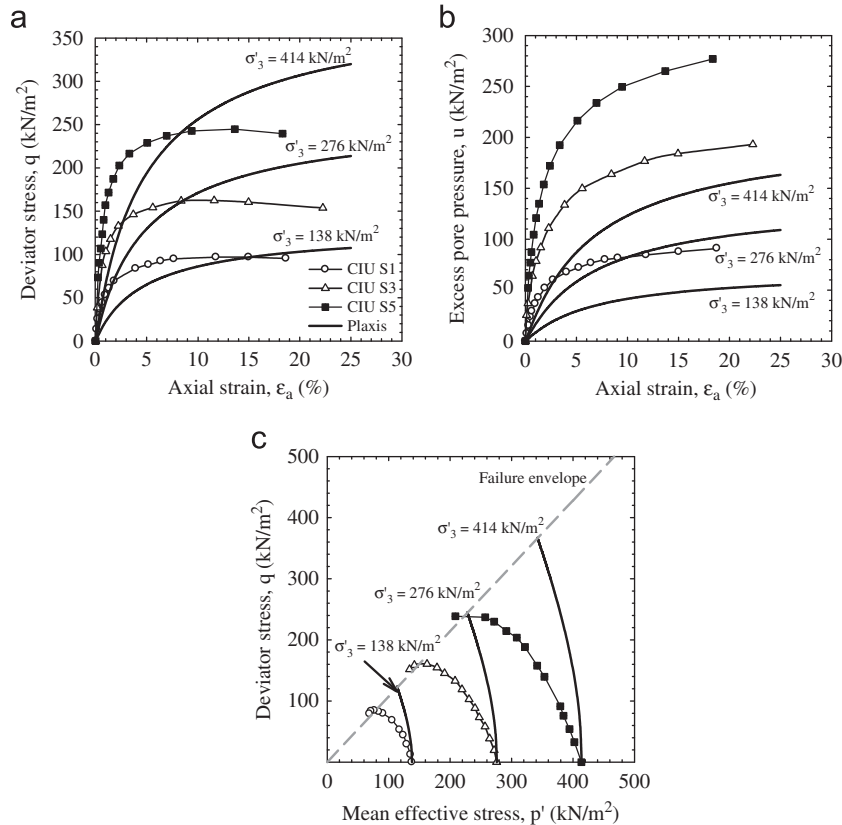


Fig. 14. Bangkok Soft Clay CIU test results and their predictions from the HSM (based on CID and Oedometer tests input parameters) (a) Deviator stress versus axial strain, (b) Excess pore pressure versus axial strain and (c) Stress path q versus p' .

shown in Fig. 15. In terms of the q versus ϵ_a and u versus ϵ_a relationships at a relatively small strain (lower than 3%), the HS Model predictions agree reasonably well with the test results. However, the HS Model cannot predict the drop in the deviator stress, which represents a strain softening. Nevertheless, in terms of an effective stress path, the typical shape of the normally consolidated clay stress paths, and their undrained shear strength, are handled very well by the HSM predictions.

5.3. HSM parameters calibration for Bangkok stiff clay

The HS Model calibration for the Bangkok stiff clay was conducted in a similar way to that used for the Bangkok soft clay. The test results from CIU F2, CIU F5 and CIU F7 ($\sigma'_3 = 69, 276$ and 414 kN/m²) were selected. The best fit HS Model parameters and their resulting predictions are illustrated in Table 8 and Fig. 16, respectively. It is noteworthy that, even with the adjusted parameters, the HS Model cannot predict the drop in the deviator stress or the excess pore pressure, with reference to their ultimate values in q versus ϵ_a and u versus ϵ_a relationships. As a consequence, if a dilatancy angle of more than zero is introduced to the HS Model, some degree of drop in the excess pore pressure would be obtained. However, with the inclusion of dilatancy, the predicted q versus ϵ_a and stress path would be unrealistic (see Schweiger, 2002).

Furthermore, it can be observed from Fig. 16(c), that the stress path q versus p' from the CIU test carried out at a confining pressure of 69 kN/m², shows heavily overconsolidated behaviour; thus, where the stress paths reach the failure envelopes (State Boundary Surface) on the dry side of the Critical State Line. These behaviours cannot be obtained from the HSM predictions. The best estimation of the HSM stress paths are the ones that are similar to the lightly overconsolidated clay, where the q versus p' stress path goes vertically up to the failure envelope. Indeed, this lightly overconsolidated behaviour is more likely to be the case for the Bangkok stiff clay as the in-situ effective vertical stress at 18 m (where stiff clay samples were taken) is about 300 kN/m².

6. Concluding remarks

In this study, the experimental data on soft and stiff Bangkok clays available in the literature was reanalysed in order to obtain the stiffness and strength parameters required for the Hardening Soil Model available in PLAXIS finite element code. Undrained behaviour of Soft and Stiff Bangkok Clays was modelled using these parameters. The following concluding remarks can be made:

- (1) For Soft Bangkok Clay; the angle of internal friction at the depths of 2.5 – 4 m can be assumed to be 26° ; this value can be reduced to 24° at depths of 5.5 – 6 m.

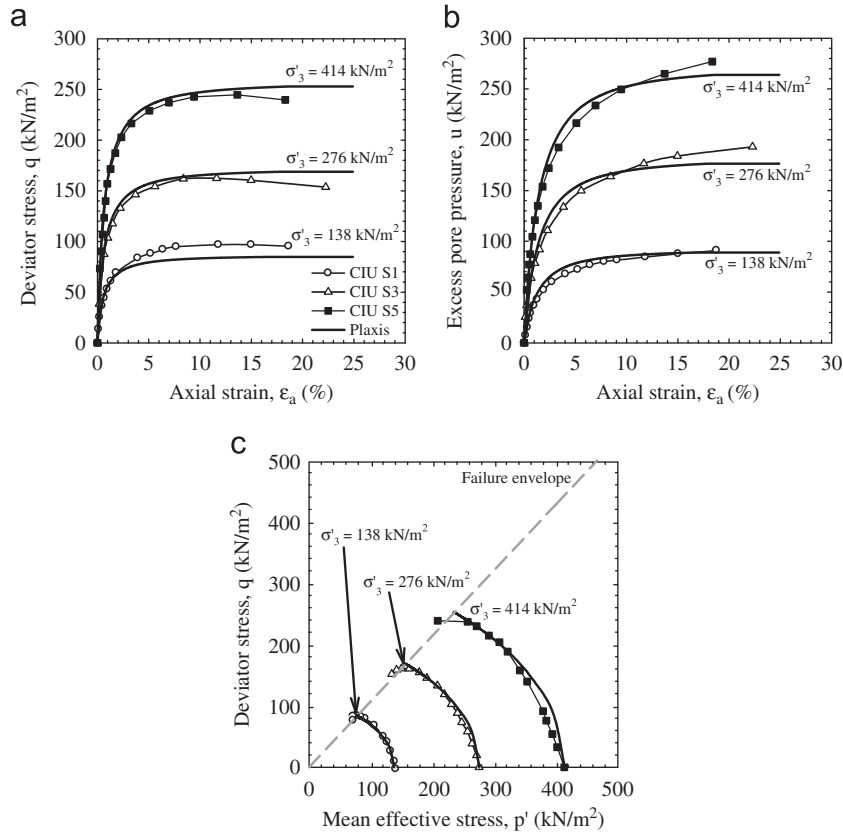


Fig. 15. Bangkok Soft Clay CIU testing results and their predictions from the HSM (Using best fit input parameters) (a) Deviator stress versus axial strain and (b) Excess pore pressure versus axial strain (c) Stress path q versus p .

For Stiff Bangkok Clay at 16 m depth, the angle of internal friction can be taken as 23° and the cohesion of 32 kN/m^2 can be used.

- (2) The reference oedometer modulus values of 962, 1,650 and $4,689 \text{ kN/m}^2$ can be assumed for soft, medium stiff and stiff clays, respectively. The corresponding values of the reference unloading/reloading oedometer modulus are 5,813, 5,394 and $9,618 \text{ kN/m}^2$. An average range of reference unloading/reloading oedometer modulus to reference oedometer loading of 2–4 is obtained for soft clay. This ratio tends to reduce with depth. The lower value approximately 1.5 is found to be appropriate for stiff clay.
- (3) The stiffness parameters required for the Hardening Soil Model were also determined from on the CIU and CID triaxial tests conducted on Soft Bangkok Clay with the confining pressures in the range from 138 to 414 kN/m^2 . From the CIU series, the initial undrained modulus and the undrained modulus at 50 per cent undrained strength range from 10.5 to 40 MN/m^2 and 5.9 to 20.5 MN/m^2 , respectively. The $E_{u,i}/E_{u,50}$ and failure ratios of 2 and 0.9 are obtained. From the CID series, the initial drained modulus and the drained modulus at 50 per cent ultimate strength range from 2.0 to 6.6 MN/m^2 and 1.0 to 2.4 MN/m^2 , respectively. The E'_i/E'_{50} ratio is approximately 2 with the failure ratio of 0.7.

- (4) Both undrained and drained moduli obtained from triaxial tests increase with the increasing confining pressure, which can be shown by double log scale plots of normalised confining pressure versus normalised undrained and drained moduli. This is consistent with the conclusions made by Janbu (1963). Furthermore, the power (m) of approximately unity is observed for all cases (undrained and drained). The reference undrained and drained moduli (at reference pressure of 100 kN/m^2) are 7.7, 4.8, 1.3 and 0.7 MN/m^2 for the cases of $E_{u,i}^{ref}$, $E_{u,50}^{ref}$, E_i^{ref} and E_{50}^{ref} , respectively. These reference moduli are readily to be used as input parameter in the Hardening Soil Model (HSM).
- (5) Similar to the triaxial test series conducted on Bangkok Soft Clay, two triaxial test series (CIU and CID) on Bangkok Stiff Clay were analysed. The confining pressure of CIU and CID series range 17 – 620 kN/m^2 and 34 – 552 kN/m^2 , respectively. For the CIU series, the initial undrained modulus and the undrained modulus at 50 per cent undrained strength ranged from 14 to 71 MN/m^2 and 4.1 to 61 MN/m^2 , respectively. The $E_{u,i}/E_{u,50}$ and failure ratios of 2.5 and 0.9 are obtained. For the CID series, the initial drained modulus and the drained modulus at 50% ultimate strength ranged from 19 to 91 MN/m^2 and 9 to 36 MN/m^2 , respectively. The E'_i/E'_{50} ratio is approximately 2 with the failure ratio of 0.9. Here

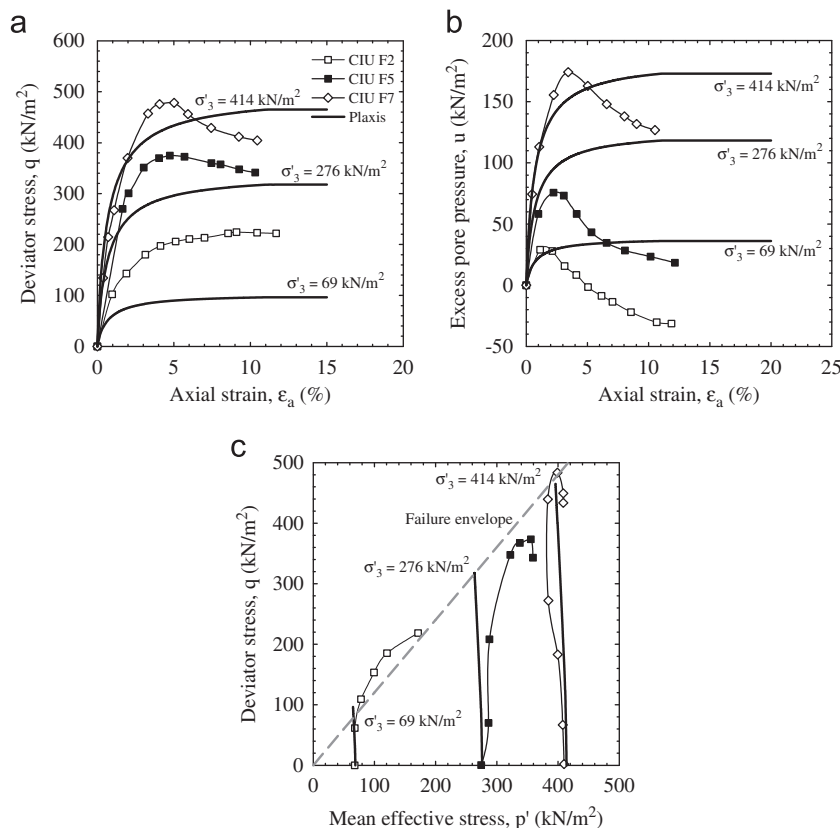


Fig. 16. Bangkok Stiff Clay CIU testing results and their predictions from the HSM (Using best fit input parameters). (a) Deviator stress versus axial strain, (b) Excess pore pressure versus axial strain and (c) Stress path q versus p .

again, a set of linear relationships is observed from the normalised double log scale plots with the power (m) of 0.5. The reference undrained and drained moduli (at reference pressure of 100 kN/m²) are 30, 11, 29 and 14 MN/m² for the cases of $E_{u,i}^{ref}$, $E_{u,50}^{ref}$, E_i^{ref} and E_{50}^{ref} , respectively.

(6) The Hardening Soil Model (HSM) parameter calibration demonstrates that the back-calculated drained moduli are needed in the PLAXIS analysis of undrained materials. Two possible reasons of this phenomenon are as follows. First, the assumption of adding bulk modulus of water, as used by the HSM in PLAXIS, to convert the drained to the undrained modulus may not be appropriate. Second, the drained moduli from CID test series may not be representative values of the Bangkok soft clay. Therefore, it is recommended that detailed process of parameter calibration is carried out in order to obtain realistic prediction of undrained behaviour of clay using PLAXIS.

Acknowledgement

The authors wish to thank the late president of the Mass Rapid Transit Authority of Thailand (MRTA), Mr. Chukiatt Phota-yanuvat and the MRTA Engineers for their kindness in encouraging and providing relevant data

for carrying out academic research activities related to such important works.

References

- Ahmed, M.A., 1976. Stress–Strain behaviour and Strength Characteristics of Stiff Nong Ngoo Hao Clay During Extension Tests Under Undrained Conditions. Master Thesis. Asian Institute of Technology, Thailand.
- AIT Research Report 91, 1981. Investigation of Land Subsidence Caused by Deep Well Pumping in the Bangkok Area.
- Al-Tabbaa, A., Wood, D.M., 1989. An experimentally based “bubble” model for clay. In: Pietruszczak and Pande (Eds.), Proceedings of the International Conference on Numerical Models in Geomechanics, NUMOG 3, Balkema, Rotterdam, pp. 91–99.
- Atkinson, J.H., Stallebrass, S.E., 1991. A model for recent stress history and non-linearity in the stress-strain behaviour of overconsolidated soil. In: Proceedings of the 7th International Conference on Computer Methods and Advances in Geomechanics, Cairns, vol. 1, pp. 555–560.
- Balasubramaniam, A.S., Hwang, Z.M., 1980. Yielding of weathered Bangkok clay. Soils and Foundations 20 (2), 1–15.
- Balasubramaniam, A.S., Chaudhry, A.R., 1978. Deformation and strength characteristics of soft Bangkok clay. Journal of Geotechnical Engineering Division, ASCE 104, 1153–1167.
- Balasubramaniam, A.S., Uddin, W., 1977. Deformation characteristics of weathered Bangkok clay in triaxial extension. Géotechnique 27, 75–92.
- Balasubramaniam, A.S., Handali, S., Wood, D.M., 1992. Pore pressure–stress ratio relationship for soft Bangkok clay. Soils and Foundations 32 (1), 117–131.

- Balasubramaniam, A.S., Hwang, Z.M., Waheed, U., Chaudhry, A.R., Li, Y.G., 1978. Critical state parameters and peak stress envelopes for Bangkok clays. *Quarterly Journal of Engineering Geology* 1, 219–232.
- Balasubramaniam, A.S., Oh, E.Y.N., Phienweij, N., 2009. Bored and driven pile testing in Bangkok sub-soils. *Journal of Lowland Technology International* 11 (1), 29–36.
- Balasubramaniam, A.S., Oh, E.Y.N., Bolton, M.W., Bergado, D.T., Phienweij, N., 2005. Deep-well pumping in the Bangkok plain and its influence on ground improvement development with surcharge and vertical drains. *Ground Improvement* 9, 149–162.
- Brand, E.W., Balasubramaniam, A.S., 1976. Soil compressibility and land subsidence in Bangkok. In: *Proceedings of the International Symposium on Land Subsidence*, Anaheim, California, USA, pp. 365–374.
- Brinkgreve, R.B.J., 2002. PLAXIS Finite Element Code for Soil and Rock Analysis—version 8. Balkema, Rotterdam.
- Chaudhry, A.R., 1975. Effects of Applied Stress Path on the Stress–Strain Behaviour and Strength Characteristics of Soft Nong Nguo Hao Clay. Master Thesis. Asian Institute of Technology, Thailand.
- Gibson, R.E., Henkel, D.J., 1954. Influence of duration of test at constant rate of strain on measured drained strength. *Géotechnique* 4 (1), 6–15.
- Gurung, S.B., 1992. Yielding of Soft Bangkok Clay Below the State Boundary Surface Under Compression Condition. Master Thesis. Asian Institute of Technology, Thailand.
- Hassan, Z., 1976. Stress–Strain Behaviour and Shear Strength Characteristics of Stiff Bangkok Clays. Master Thesis. Asian Institute of Technology, Thailand.
- Hwang, Z.M., 1975. Stress Strain Behaviour And Strength Characteristics of Weathered Nong Nguo Hao clay. M.Eng. Thesis. AIT, Bangkok, Thailand.
- Janbu, N., 1963. Soil compressibility as determined by oedometer and triaxial test. In: *Proceedings of the European Conference on Soil Mechanics and Foundation Engineering*, pp. 19–25.
- Kerdsuwan, T., 1984. Basic properties and Compressibility Characteristics of First and Second Layers of Bangkok Subsoils, M.Eng. Thesis. AIT, Bangkok.
- Kim, S.R., 1990. Stress–Strain Behaviour and Strength Characteristics of Lightly Overconsolidated Clay. Ph.D. Thesis. Asian Institute of Technology.
- Kondner, R.L., 1963. Hyperbolic stress–strain response cohesive soils. *Journal of Soil Mechanics and Foundations Division*, ASCE 89, 115–143.
- Koslanant, S., 1997. Consolidation Characteristics of Soft Bangkok Clay using Constant Rate of Strain Consolidometers, Master Thesis no. GE-96-15. Asian Institute of Technology, Bangkok, Thailand.
- Li, Y.G., 1975. Stress Strain Behaviour and Strength Characteristics of Soft Nong Nguo Hao Clay, M.Eng. Thesis, AIT, Bangkok, Thailand.
- Nanegrungsung, B., 1976. Consolidation Characteristics of Pathumwan Clay. Thesis 900, AIT, Bangkok.
- Nordal, S., 1999. Present of Plaxis. Beyond 2000 in *Computational Geotechnics-10 Years of PLAXIS International*. Balkema, Rotterdam, pp. 45–54.
- Roscoe, K.H., Burland, J.B., 1968. On the generalised stress-strain behaviour of wet clay. *Engineering Plasticity*, 535–609.
- Schanz, T., Vermeer, P.A., Bonnier, P.G., 1999. The hardening soil model: formulation and verification, Beyond 2000 in *Computational Geotechnics*. Balkema, Rotterdam.
- Schweiger, H.F., 2002. Some remarks on pore pressure parameter A and B in undrained analyses with the Hardening Soil Model. *PLAXIS Bulletin* 12, 6–9.
- Schweiger, H.F., 2009. Influence of constitutive model and EC7 design approach in FEM analysis of deep excavations. In: *Proceeding of ISSMGE International Seminar on Deep Excavations and Retaining Structures*, Budapest, pp. 99–114.
- Shibuya, S., Tamrakar, S.B., Manakul, W., 2003. Geotechnical hazards in Bangkok—present and future. *Journal of Lowland Technology International* 5, 1–13.
- Sinsakul, S., 2000. Late quaternary geology of the lower central plain, Thailand. *Journal of Asian Earth Sciences* 18, 415–426.
- Soos von, P., 2001. Properties of Soil and Rock (in German), *Grundbau-taschenbuch*, vol. 1, 6th Ed., Ernst and Son, Berlin, pp. 117–201.
- Surarak, C., 2010. Geotechnical Aspects of the Bangkok MRT Blue Line Project. Ph.D. Thesis. Griffith University, Australia.
- Tonyagate, W., 1978. Geotechnical Properties of Bangkok Subsoils for Subsidence Analysis. Thesis 1298. AIT, Bangkok.
- Whittle, A.J., Kavvadas, M.J., 1994. Formulation of MIT-E3 constitutive model for overconsolidated clays. *Journal of Geotechnical Engineering*, ASCE 120 (1), 173–198.
- Wood, D.M., 1995. Kinematic hardening model for structure soil. In: *Pande and Pietruszczak (Eds.), Proceedings of the International Conference on Numerical Models in Geomechanics NUMOG 5*, Balkema, Rotterdam, pp. 83–88.